Article:

Lin, G., Fan, C. orcid.org/0000-0001-5684-2547, Fu, Z. et al. (6 more authors) (2025) Insight into the instability of ammonia-methane laminar diffusion flame. Journal of the Energy Institute, 119. 101961. ISSN 1743-9671

https://doi.org/10.1016/j.joei.2024.101961

Insight into the instability of ammonia-methane laminar diffusion flame

Guorong Lin[a], Chenyang Fan[a*], Zheng Fu[a,b], Haizhao Li[a], Ye Liu[c*], Huiyong Du[a], Bin Xu[a], Shuo Jin[a], Mingliang Wei[b]

[a] Henan Provincial International Joint Laboratory of Energy Conservation and Pollutant Control of Energy Power Equipment, College of Vehicle and Traffic Engineering, Henan University of Science and Technology, Luoyang 471003, China

[b] State Key Laboratory of Intelligent Agricultural Power Equipment, Luoyang 471003, China

[c] Institute for Transport Studies, University of Leeds, Leeds LS2 9JT, UK

Corresponding author: Chenyang Fan

E-mail address: fanchenyang@haust.edu.cn; fanchenyang@tju.edu.cn

Postal address: College of Vehicle and Traffic Engineering, Henan University of Science and Technology, Luoyang 471003, China

Abstract

Ammonia is one of carbon-neutral hydrogen derivatives and is identified as a sustainable fuel for mobile applications. However, the combustion instability of pure ammonia remains a significant challenge. In this study, the combustion instability of ammonia flame with methane as a combustion promoter was investigated using high-speed photography and schlieren techniques on ammonia-methane-air co-flow laminar diffusion flames. It was found that after exceeding a threshold of fuel flow rate (Q_f), the stable laminar flame turned to a regular and reproducible oscillation, accompanying by periodic bulging and separation of the flame. The addition of co-flow air increases flame flickering frequency, which can be reduced by increasing the Q_f. In contrast to the pure methane diffusion flame with distinct luminous zones, the NH_3/CH_4 diffusion flame exhibits a reddish-orange color with no distinguishable luminous zone. Additionally, the addition of ammonia shrinks the appearance of flames, and slightly decreases the flame flickering frequency at 30% substitution, while increases it at 50% substitution. A spindle-shape shear layer between the flame and the surrounding air, exhibiting periodic motion during the flickering sequence. The addition of ammonia decreases the maximum shear layer diameter and increases its motion velocity. The co-flow air pushes the vortex formation location downstream, reducing fluctuation amplitude of the shear layer. Ammonia substitution further promotes this downstream shift, potentially lessening the flame flickering.

Keywords: Ammonia fuel; Flame flickering; Laminar diffusion flame; Schlieren technique; Shear layer

Nomenclature

Re	Reynolds number
Fr	Froude number
Q_f	Fuel flow rate (SLPM)
v_{cf}	Co-flow air rate (SLPM)
f	Flame flickering frequency (Hz)
α_N	Ammonia volume ratio
H_{max}	The maximum flame height (mm)
H_{min}	The minimum flame height (mm)
w_s	Flame width (mm)
H_p	Height of blue zone (mm)
w_p	Width of blue zone (mm)
d_s	Diameter of shear layer (mm)
v_s	Motion velocity of shear layer (m/s)
H_v	Height of maximum diameter shear layer (mm)

1. Introduction

Dependence on fossil fuels has worsened carbon dioxide emissions and environment pollution [1]. Ammonia, a carbon-free fuel with no direct greenhouse effect, has emerged as a leading candidate to mitigate environmental problems [2]. Additionally, as an excellent hydrogen carrier, ammonia exhibits a greater energy density while requiring substantially lower pressure relative to hydrogen, providing greater safety [3-5]. However, due to its disadvantages, including slow combustion rate and elevated NO_x emissions, direct application of ammonia on engines is challenging. A potential way to circumvent ammonia's disadvantages is to operate the engine using the mixture of ammonia-methane as fuel [6-9], due to the significant enhancement of burning velocity by methane across a broad spectrum of equivalence ratios and ammonia concentration [10].

The dual fuel combustion mode of ammonia/methane in engines has been widely studied. Huang et al. [11] reported that NO_x emission was gradually reduced as ammonia energy ratio rose from 0% to 30% in a free-piston engine generator. The study of Wei et al. [12] on a marine dual-fuel engine using natural gas and ammonia also demonstrated that as the ammonia blending ratio increases, total NO_x emissions decrease under stoichiometric conditions. While reduction in NOx emissions is favorable, maintaining flame stability becomes increasingly challenging as ammonia ratios rise. The stable flame operating region narrowed as the ammonia ratio increased [13]. In the study of Ku et al. [14] on counterflow non-premixed flame, flame extinction occurred at a strain rate of approximately 540 s^{-1} for pure methane flame. As ammonia substitution increased, extinction strain rate decreased, with a reduction of about 78% at an ammonia ratio of 0.9. A similar tendency was observed by Chu et al. [15]. Thus, to better utilize ammonia, a deeper understanding of combustion characteristics of ammonia/methane mixtures is imperative.

As an essential combustion characteristic, the combustion instability has received considerable attention. Ariemma et al. [13] investigated the instability limits in relation to the equivalence ratio and the composition of ammonia-methane fuel in the Laboratory Unit CYclonic (LUCY) burner. The results showed that the stable operational range of NH_3/CH_4 premixed flame was extended compared to pure ammonia. Khateeb et al. [16] studied the instability limits of ammonia-methane-air mixtures across a broad spectrum of ammonia blending ratio in a laboratory-scale generic swirl burner. They found that as ammonia substitution increased, the equivalence ratio at the lean blowout limit increases but also the tendency for flame flashback to decrease. Nevertheless, their research focused on the premixed flames, while studies on instability in laminar diffusion flames remain limited.

Although turbulent combustion is widely applied in industry, it is difficult to study experimentally due to its motion with high level of intermittency and relatively short residence time [17, 18]. According to laminar flamelet model, a turbulent diffusion flame consists of a collection of laminar diffusion flamelets [19], thus comprehending laminar diffusion flame instability is significant for industrial application. In laminar diffusion flames, the flame instability can be reflected by the condition in which flickering phenomenon occurs. When the Froude number is sufficiently low, a jet flame shows a periodic jump state, commonly known as flickering [20].

Flame flickering is commonly observed in laboratory-scale experiments [21, 22]. Relevant studies prove that the flame flickering is associate with the flame feature, such as its height and width, as well as the generation and dynamics of vortices. The results of Kimura [23] and Durox et al. [24] indicated that flame flickering was correlated with flame height, and there was a minimum flame height required to cause flickering. Zhang et al. [25] found the similar phenomenon. Their results showed that with an increase in oxygen concentration of co-flow air, the flame height was diminished, thereby stabilizing the flame. Furthermore, the study by Ge et al. [26] indicated that the vortices formed above the flame reaction zone, contributing to the flame stability. Wang et al. [27] investigated the vortex dynamics and structures in methane-air co-flow diffusion flame using high speed direct and schlieren imaging system. The results showed that the velocity of co-flow air had a significant impact on the dynamics of the vortices outside the visible flame. Piemsinlapakunchon et al. [28] presented a numerical study on the crucial impact of syngas composition and air co-flow on laminar diffusion flame instability. They revealed that a high content of H_2 resulted in low instability, while a higher proportion of CH_4 increased the level of instability. In addition, the flame instability was suppressed by the addition of co-flow.

Fuel type is also a significant factor on flame flickering. Gohari Darabkhani et al.

[29] found that there are three dominant flickering frequency in a ethylene diffusion flame in contrast to methane diffusion flame with one dominant flickering frequency. The results of Li et al. [30] showed that the pure methane and propane diffusion flames exhibited little variation, with peak frequencies at 11—13 Hz. However, a peak flickering frequency at 6 Hz was observed in the case of a ratio of a 1:1 mixture.

The afore-discussed studies focused on flickering of hydrocarbon fuel co-flow diffusion flame. The flames of ammonia-containing fuels, which is believed to possess distinctly different structure and kinetics, may present a different instability phenomenon. For example, Nourani Najafi et al. [31] found that increasing the ammonia fraction decreased the height of the flame and the proportion of yellow luminous zone, while reddish-orange luminous zone progressively replaced blue zone at the base of flame. Zhang et al. [32] reported that as the ammonia blend ratio increased, the flame height grew and the pyrolysis region (dark brown luminous zone) extended considerably. On the other hand, upstream of flame temperature along centerline decreased while downstream temperature rose in response to the higher ammonia blend ratio. It is in agreement with the results reported by Ren et al. [33]. Cheng et al. [34] found that doping ammonia into n-decane increased flame height and had an impact on flame temperature. The flame instability for ammonia-containing fuels has been preliminarily assessed in the research conducted by Colson et al.[35] and Yang et al. [36]. Colson et al. [35] examined flame-burner interactions and the influence of ammonia substitution on the stabilization mechanisms of the attached flame in a non-premixed methane jet flame. The results showed that the flame position (the distance from the base to the burner) shifted downstream due to ammonia substitution. They focused on flame liftoff and highlighted the perturbation caused by ammonia substitution on the stabilization dynamics before liftoff, but did not describe the overall flame stability. Yang et al. [36] explored the flickering behavior of NH_3/CH_4 laminar diffusion flames with a constant co-flow air rates in low-pressure. It was found that the reduction in pressure eased vortex formation and weakened its interaction with the flame. The ammonia substitution slowed vortex formation. The impacts of pressure and ammonia substitution on flickering were emphasized, while the influence of co-flow air rates on flickering, as afore-discussed, was not taken into account.

Therefore, further investigations on flame instability for ammonia-methane fuel is of great necessity. In present study, high-speed direct imaging combined with schlieren methods were utilized to examine the flickering flame and the evolution of outer vortex under varying fuel compositions and air co-flow rates. The present work may help the further understanding of ammonia combustion and enrich the database of combustion mechanisms.

2. Experimental set-up

In the present work, a laminar diffusion flame was produced by a McKenna Products flat-flame burner with a fuel nozzle exit diameter of 8 mm, surrounded by a 60 mm diameter coaxial air annulus. The burner contained an Archimedean spiral cooling circuit for water flow to minimize radial temperature gradients. The fuel/air co-flow system was placed in an acrylic cover to mitigate environmental interference. The flow rates of methane and ammonia were measured and mixed by mass flow controllers (AB-11, AiroBoost) with an accuracy 1% of full scale. Tab. 1 shows the test conditions of the experiment. The fuel flow rates (Q_f) ranged from 0.3—0.5 slpm (standard liters per minute). The co-flow air rates (v_{cf}) varied in 0—15 slpm.

Tab. 1 Test conditions.

Conditions	Fuel flow (SLPM) Q_{CH4}	Fuel flow (SLPM) Q_{NH3}	Ammonia ratio α_N	Air flow (SLPM)	R_e	F_r
M1	0.3 (9.95 cm/s)	/	/		46.6	0.126
M2	0.4 (13.27 cm/s)	/	/		62.2	0.225
M3	0.5 (16.59 cm/s)	/	0	0—15 (0—15.16 cm/s)	77.7	
M4	0.35	0.15	0.3		81.4	0.351
M5	0.25	0.25	0.5		84.1	

The experimental set-up is shown in Fig. 1. A high-speed camera (Memrecam GX-8, NAC) was used to capture the evolution of flame structure. All flame images (1024 × 1024 pixels) were recorded at a framing rate of 1000 fps, and the shutter speed was set at 1/2000 s. Capturing accurate images of the flame and ensuring the reproducibility of experiments requires that the photographic parameters remain consistent, even though the flames become dimmer due to the addition of ammonia. A Z-type schlieren imaging system (HGD-SD200) mainly consists of a 300W Halogen Tungsten lamp and two concave mirrors. The Halogen Tungsten lamp was employed due to its continuous spectrum in the visible range, providing stable and broad light output. Each mirror has an effective diameter of 200 mm and a focal length of 2000 mm. It was used to investigate the evolution of hot gas and its interaction with v_{cf}. For all tests, the schlieren images were recorded at the same frame rate and shutter speed with the direct imaging method. The results were obtained by averaging five circulations selected from 2,000 pictures for each case. The error bars correspond to the uncertainty in flame size measurement, and are represented in red. Only results obtained from flame flickering are provided.

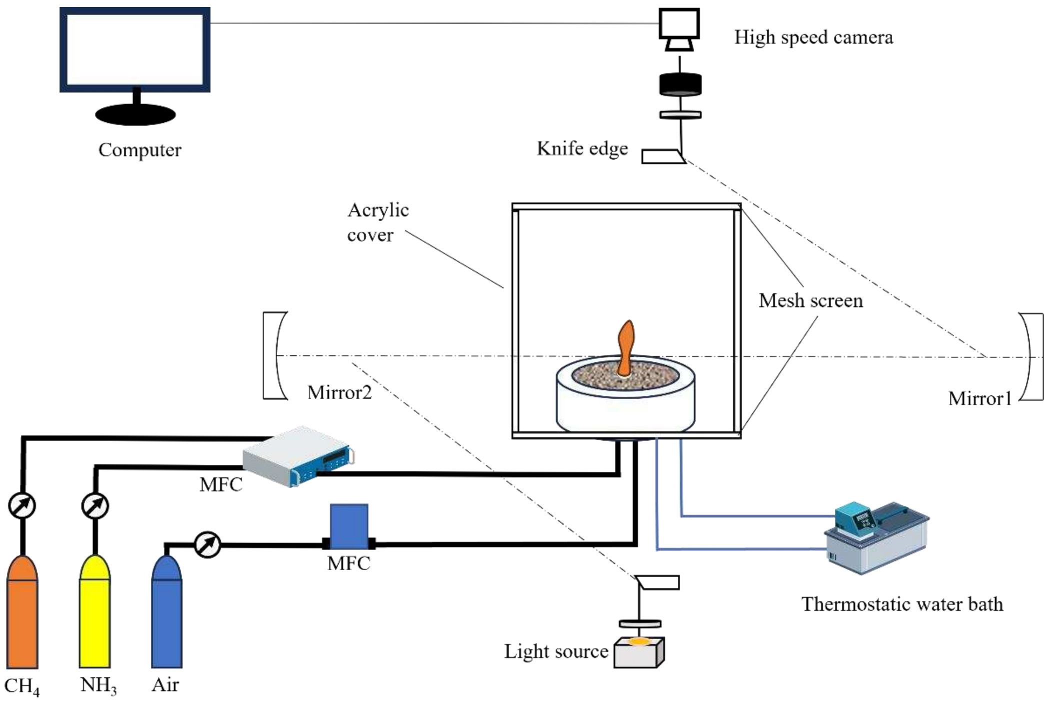

Fig. 1 Experimental set-up.

3. Results and Discussion

3.1 Flame Flickering

3.1.1 Methane diffusion flame

For a certain burner configuration, the stability of co-flow diffusion flame primarily relies on the fuel formulation, co-flow type, flow rates, and the ambient pressure [29]. The flame flickering at three flow rates of fuel and with various v_{cf} conditions is examined in this study. With no additional co-flow gas, the threshold of Q_f for the stable flame is 0.16 slpm. When further elevating the Q_f, the flame flickering occurred. A complete sequence of high-speed images depicting methane-air diffusion flames at various Q_f and v_{cf} is presented in Fig. 2, in the time resolution of 0.014 s. It was observed that the flames exhibit consistent and repeatable oscillation. Initially, the main change is observed at the tip of flame. Then, changes are noted at both the flame tip and neck, eventually leading to necking which separates the bulged portion of the flames. Similar phenomenon has also been observed in the study of Gohari Darabkhani et al. [37] on a laminar co-flow methane diffusion flame. They assigned this phenomenon to the circinate vortex beneath the flame bulge pushes the flame surface outward, while the vortex over the bulge pulls the surface inward, enhancing the blending of fuel and air at certain moments. Consequently, the local combustion rate increases, causing part of the flame tip to neck and quench.

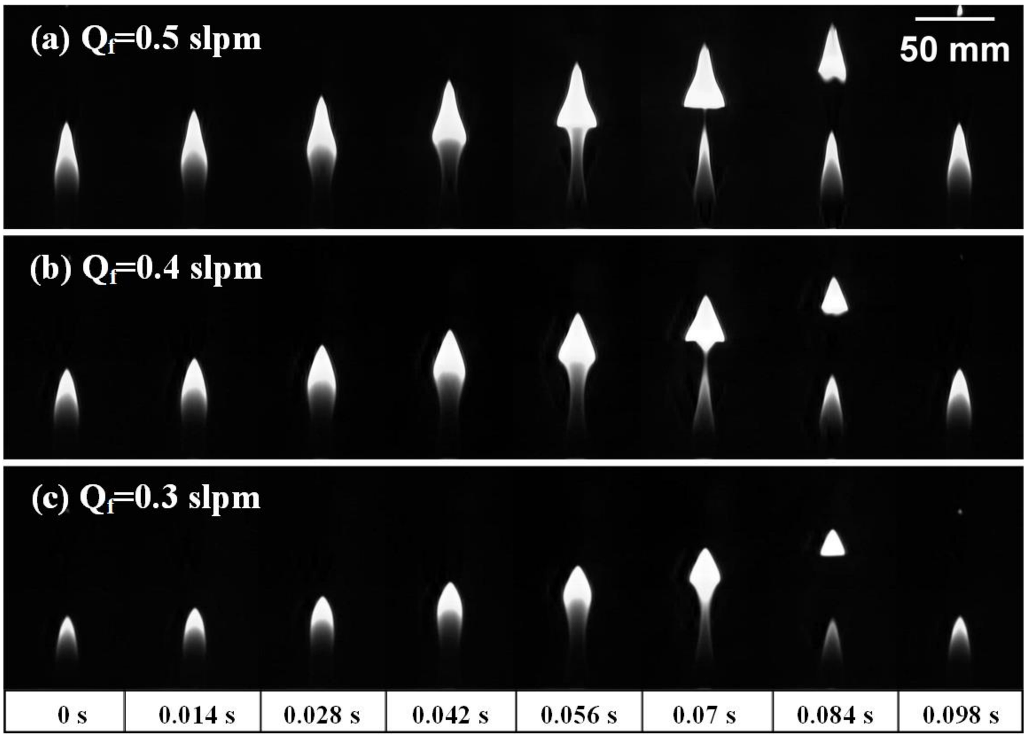

Fig. 2 Whole sequences of high-speed images of the pure methane (0.5, 0.4, 0.3 slpm) flames without additional co-flow gas.

The flickering frequency of the flame is obtained through Fast Fourier Transform (FFT) analysis of the mean brightness intensity from 2000 high-speed photographs of the flame, sampled at a rate of 250 Hz [38]. The flickering frequency (*f*) of methane-air diffusion flame at various flow rates is presented in Fig. 3. The *f*, in a range of 10—13 Hz, rises with increasing v_{cf}, while it decreases as the Q_f increases. The results are similar to the findings of Fujisawa et al. [39]. They found two modes of flickering frequency in the methane diffusion flame. The lower flickering frequency, ranging from 10 to 12 Hz, represents the fundamental mode of the flickering flame and gradually increases as the v_{cf} rises. In contract, the higher flickering frequency remains nearly constant at 17 Hz, regardless of the v_{cf}. In summary, the increase in flow rates of v_{cf} increases the flickering frequency while the increase in Q_f decreases it.

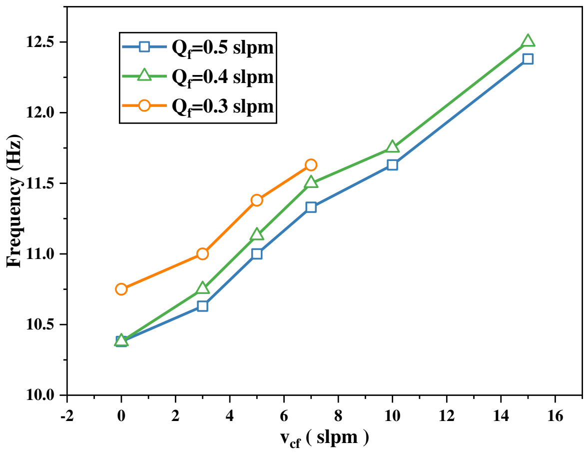

Fig. 3 Frequency of flickering flame at different fuel flow rates (Q_f) and co-flow air rates (v_{cf}).

To facilitate a clearer observation of the flame changes with v_{cf}, flame dimensional parameters are extracted from the flame images, and the definitions are depicted in Fig. 4. The maximum height (H_{max}) denotes the highest point the visible flame tip above the burner before separation of the bulged section. The minimum height (H_{min}) is defined as the lowest height of the flame body tip, after the separation of the bulged section in the flickering flame [25]. The flame width (w_s) referred to the maximum width of the separated part of the flame. These results are shown in Fig. 5. It is observed that increasing flow rates of the v_{cf} increases H_{max} and decreases w_s. The H_{max} initially increases with increasing v_{cf}, but later declines. It is speculated that the higher v_{cf} enhances the velocity gradient in the shear layer, which in turn enhances the stretching, finally leading to increased flame height and reduced width of the separated part of the flame.

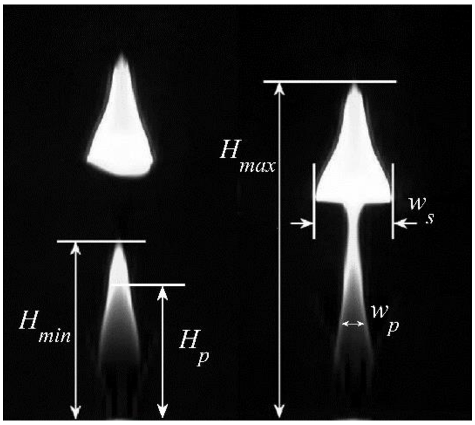

Fig. 4 Definitions of flame dimensional parameters.

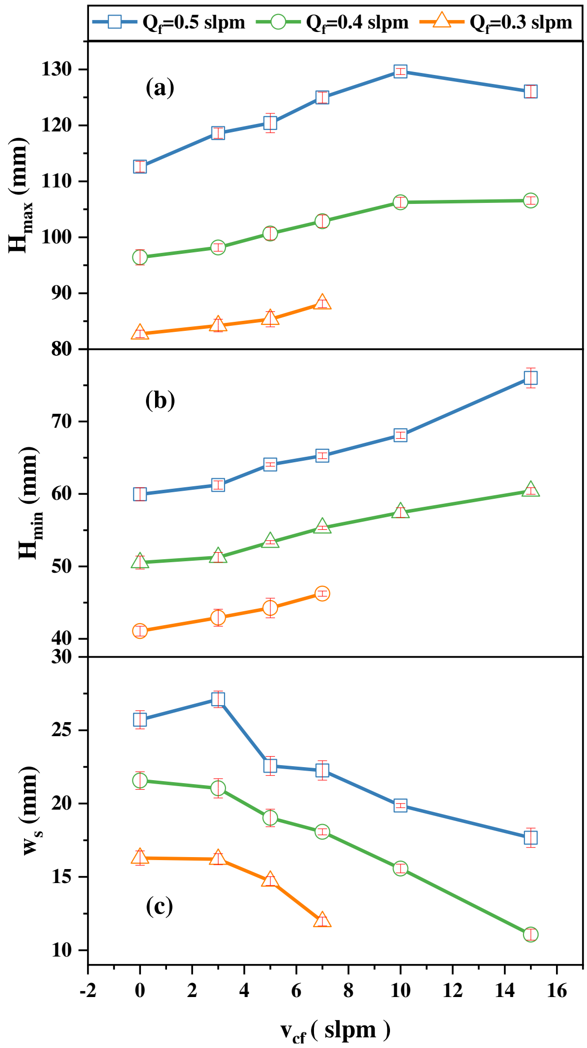

Fig. 5 The pure methane diffusion flame dimensional parameters at various rates of fuel (Q_f) and co-flow air (v_{cf}): (a) the maximum flame height (H_{max}); (b) the minimum flame height (H_{min}); (c) the width of separated flame part (w_s).

Through further scrutinization on the flame images, it is found that the methane diffusion flame exhibits two characteristic zones [40]: a blue-green zone primarily located in the premixed flame region, which aligns well with the CH* and C2* chemiluminescence intensities; a typical yellow-reddish flame owing to the solid carbon/soot emission, representing the non-premixed flame region. To depict the two zones, the original flames images were post-processed using the method as follows: the original images were first converted to grayscale to simplify the data processing and emphasize the brightness information without the influence of color [41]. Subsequently, a colormap was applied to the grayscale images to visually represent the brightness values. The colormap images depicting methane (0.5 slpm) diffusion flames under rising v_{cf} are shown in Fig. 6. The region where brightness value is greater than 150 is considered the yellow-reddish zone, and the blue-green zone is represented by a brightness value of less than 100. As a function of time, the brightest zone in flame body initially grows and then separates, leaving a small part in the flame body, as denoted by the yellow dotted line in Fig. 6. As the v_{cf} increase, the part left of the brightest zone in flame body also increases. The phenomenon may result from that the location of the vortex formation moves downstream due to the increase in v_{cf}, causing the vortex to be taken away the flame tip. The vortex beneath the flame tip entrains the polycyclic aromatic hydrocarbons (PAHs) downstream, which are known to be precursors to soot formation [42, 43], leading to a number of soot forming in the separation part. Thus, the separation part possessing more areas of brightest region. When the location of the vortex formation rises, the weakened entrainment results in the more areas of brightest region in flame tip. A similar phenomenon was found in the studies by Darabkhani [37] and Fujisawa et al. [38]. Darabkhani et al. conducted a quantitative analysis of the length of the separated part. The length was maximum without co-flow and gradually decreased with increasing co-flow. It was attributed to the reduced influence of vortices on the flame after the vortices were pushed downstream by co-flow.

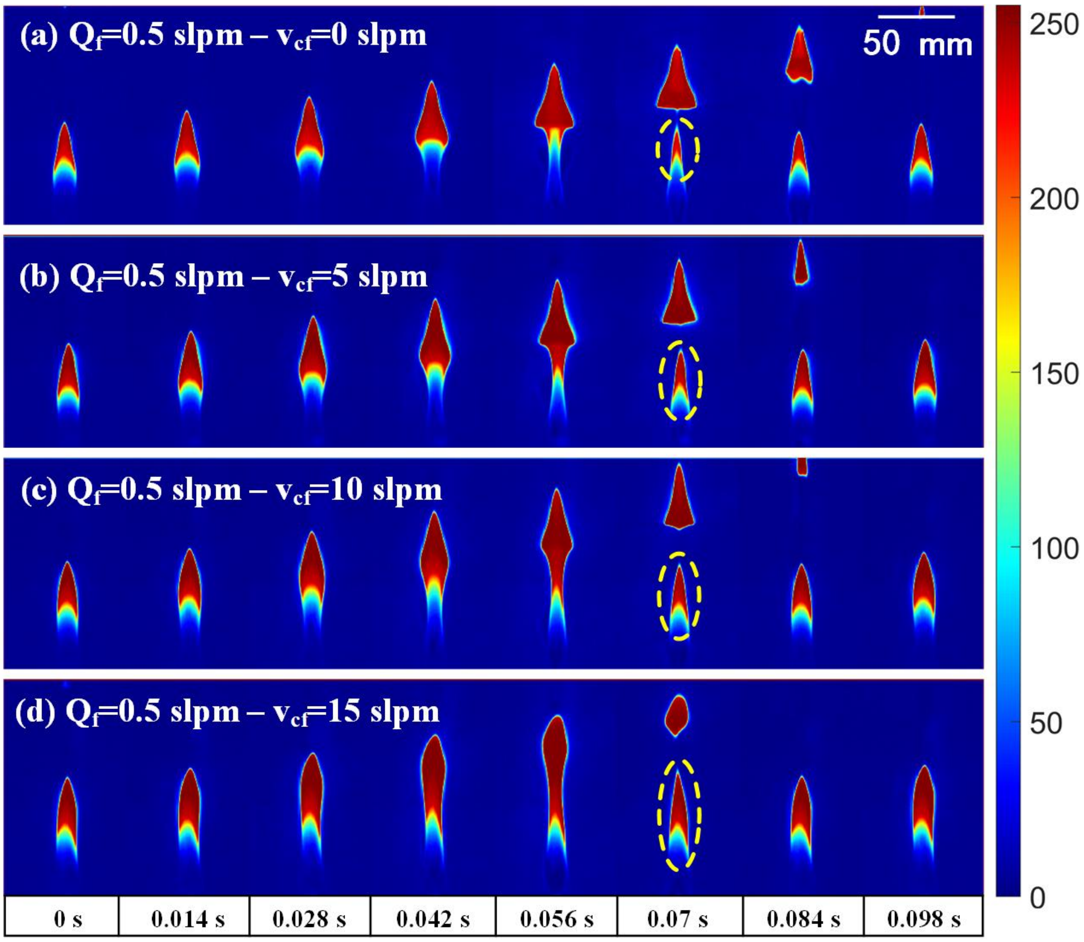

Fig. 6 Whole sequences of colormap images of methane (0.5 slpm) diffusion flames with increasing co-flow air rates (v_{cf}).

According to Fig. 6, it is observed that the periodic variations occurred not only in the yellow-reddish zone but also in the blue-green zone. This means that both physical and chemical properties of flame occur changes in flickering. It is significant to pay attention to the changes of the blue-green zone for understanding flame instability. The variation of blue-green zones is shown in Fig. 7. H_p is defined as the height of blue-green zone (partially premixed region), and w_p is width at the half height of visible edge between yellow-reddish and blue-green zone, as shown in Fig. 4. As the Q_f increases, both w_p and H_p rise. As illustrated in Fig. 7(a) and (c), w_p initially descends to a valley point and then ascends to a level comparable to its initial value with elapsed time, while H_p increases and then decrease. The maximum oscillation amplitude of w_p is 7.56 mm that is far less than that of H_p (19.27 mm). It is suggested that the area of the partially premixed region initially extends and then diminishes. While more oxidizer entrains into fuel, causing the increase in the area of the partially premixed region. It is reasonable to speculate that the chemical kinetics in the flame have changed during the flickering period. It is evident from Fig. 7(b) that the oscillation amplitude of w_p diminishes with the increase in v_{cf}. The evolution of H_p with v_{cf} in Fig. 7(d) suggests that increasing v_{cf} caused the valley point to occur earlier. The flame goes through the stretching and necking before the valley point, after which it begins to separate. The earlier occurrence of the valley point reflects the change in the flickering period.

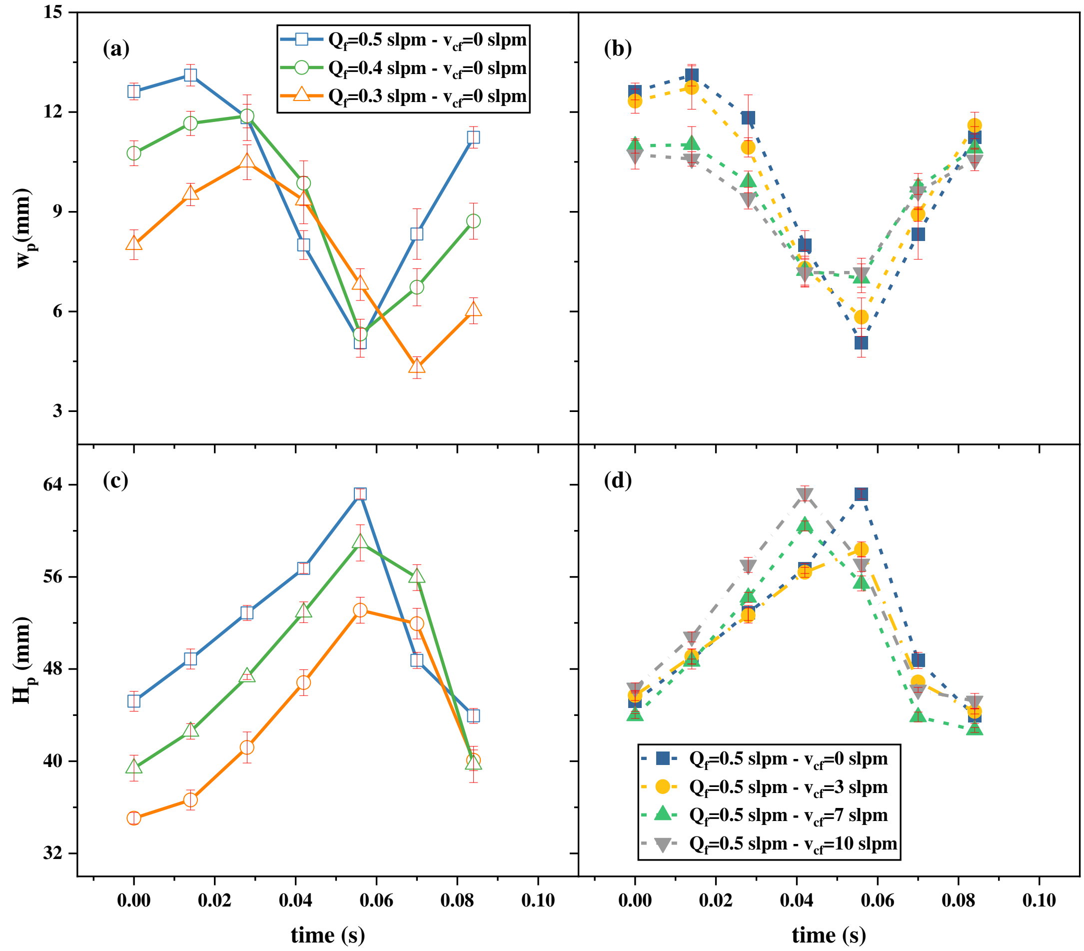

Fig. 7 Variation of blue-green zone over time; (a) the width at the half height of visible edge for blue-green zone (w_p) with various fuel flow rate (Q_f) without co-flow air; (b) w_p with various co-flow air rates (v_{cf}); (c) the height of blue-green zone (H_p) with various Q_f without co-flow; (d) H_p with various v_{cf}.

3.1.2 Ammonia-methane diffusion flame

For assessing the impact of ammonia substitution on a methane diffusion flame, experiments with NH_3/CH_4 diffusion flames at various ammonia blend volume ratios (α_N) have been conducted at the constant Q_f of 0.5 slpm. The appearance of the NH_3/CH_4 flame resembles the pure methane flame at the Q_f of 0.3 slpm, as shown in Fig. 8. The bulged section of the NH_3/CH_4 flame shows a more rounded shape in contrast to the angular shape of the pure methane flame at 0.5 slpm. As discussed above, the bulge and separation are a consequence of the effect of the vortex on the flame surface. This observation implies that the introduction of ammonia alters the interaction between flames and surrounding air.

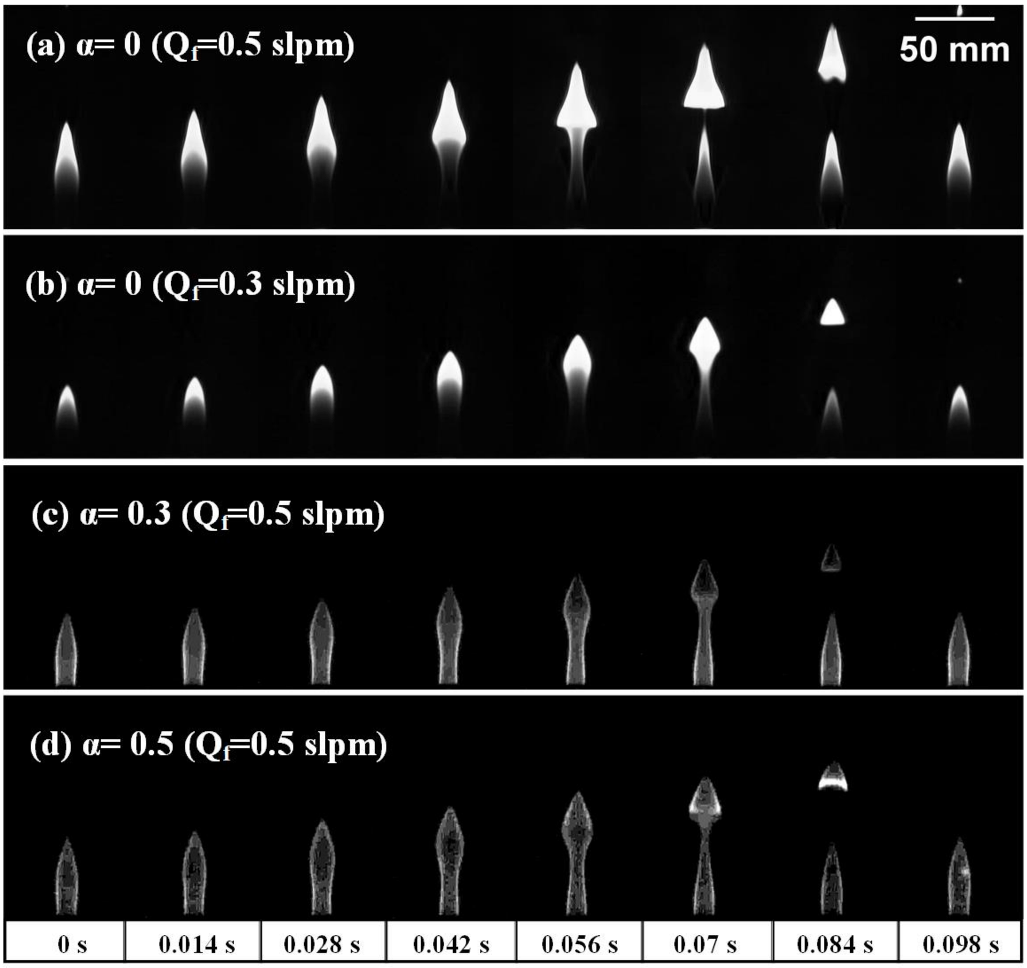

Fig. 8 Whole sequences of high-speed images of NH_3/CH_4 (ammonia volume ratio, α_N= 0, 0.3, 0.5) flame without additional co-flow gas.

The NH_3/CH_4 diffusion flame exhibits a flickering phenomenon resembling the pure methane diffusion flame. Fig. 9 shows the frequency of flame flickering at various ammonia ratios and v_{cf}. The flickering frequency rises as v_{cf} rate increases in all ammonia ratios. As shown in Fig. 9, for α_N=0.3, the flame possesses a sharp increase with the increasing v_{cf} less than 10 slpm and then slightly increases as the co-flow rate further increases, in the flickering frequency. This phenomenon is consistent with the study on a methane flame of Fujisawa et al. [39]. Their findings showed that there was a surge in flickering frequency with increasing co-flow flow rate, after which the frequency exhibited slight changes. The sharp jump occurred at higher co-flow rates as the Q_f increased. A similar phenomenon was noted in the study of Zhang et al. [44] on a methane diffusion flame, and was assigned to the fact that the downstream moving of the earliest outer vortex ring core, closely linked to the initiation of outer shear layer instability. Moreover, it is widely recognized that the flickering in a laminar flame is driven by buoyancy [45], which arises from the discrepancy between density gradient and gravitational vectors [46]. The addition of ammonia alters the fuel composition and then the changes of density gradient in the shear layer at the interface of flame and surrounding air, thereby altering the interaction between the fuel and the surrounding environment. This fact may be another plausible factor for the earlier sharp jump ending in the NH_3/CH_4 flame at α_N=0.3. The flame flickering frequency at α_N=0.5 also increases with v_{cf}. However, the flame tends to a stability with v_{cf} further increases to >10 slpm, according to the disappearance of stretching, necking and tip expansion of the flame. This may be due to the height of the visible flame being less than that of the location of the vortex formation, as discussed in Section 3.2.

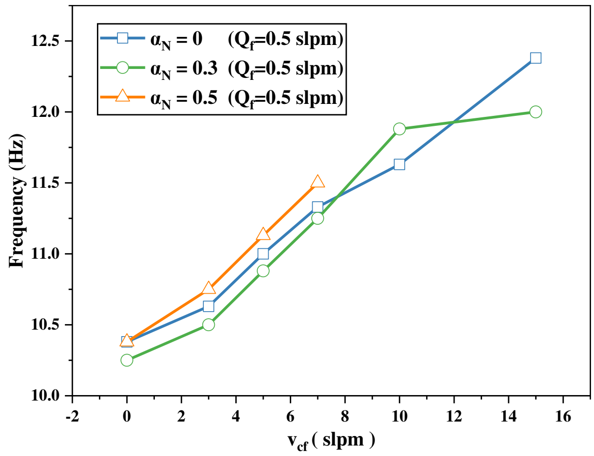

Fig. 9 The frequency of flickering flame at different ammonia ratios and co-flow air rates (v_{cf}).

The results of dimensional parameters for the flame with ammonia substitution are shown in Fig. 10. The variations of dimensional parameters as a function of v_{cf} are similar to that of the pure methane flame, but the values of dimensional parameters are below those of the pure methane flame. Notably, the H_{min} of the flame at α_N=0.3 shows a sharp increase with increasing v_{cf} up to 10 slpm and then decreases. This may be attributed to a shift in the flickering behavior of the NH_3/CH_4 flame at the v_{cf} of 10 slpm, as illustrated in Fig. 11. In this case, the flame tip stretches and then shortens rather than separates as the time elapses. This phenomenon is agreement with the study of Yang et al. [47] on a methane diffusion flame at sub-atmospheric pressure. They found that the oscillation amplitude of the flame (the difference between H_{max} and H_{min}) decreased significantly with dropped pressure, responsible from the inhibition of flame flickering in low-pressure conditions. Although the Q_f is constant, the appearance of the flame shrinks due to the addition of ammonia. Najafi et al. [31] also observed changes in flame structure caused by ammonia substation in methane flames and used nitrogen for comparison. They found that the flame height decreased with increasing substitution ratio for both nitrogen and ammonia. According to the simple Burke-Schumann theory [48], it is speculated that the shrinkage of the flame results from the reduced stoichiometric air demand for fuel, in turn decreasing mixing time required to achieve stoichiometric mixture, which can be used to explain the decrease in both flame height and width by ammonia addition. This can also be evidenced from another perspective by the elongation of flame with increasing ammonia substitution in ammonia-hydrogen flames [49]. The ammonia substitution in hydrogen flames increased the overall stoichiometric air demand. Because ammonia requires more oxygen for complete combustion compared to hydrogen.

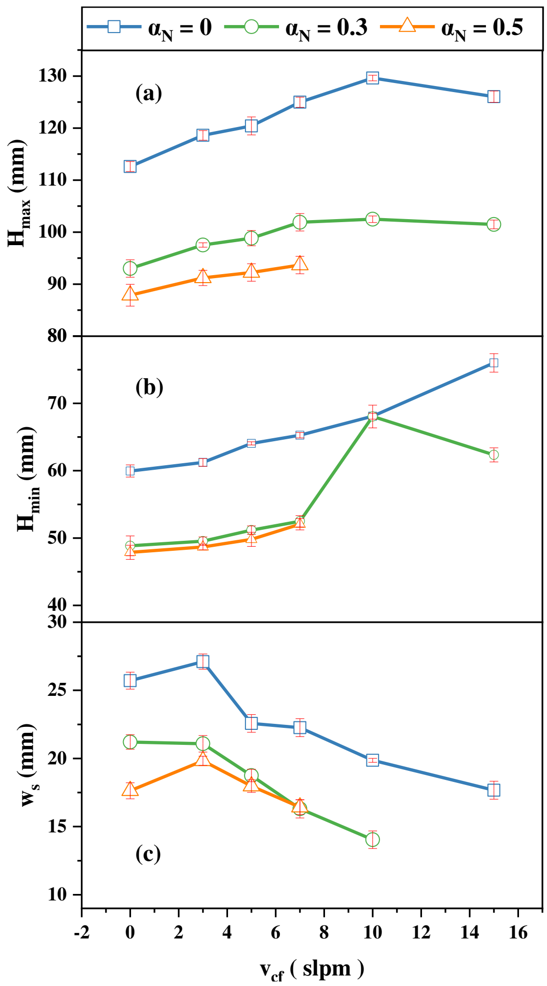

Fig. 10 NH_3/CH_4 diffusion flame dimensional parameters at various ammonia ratios and co-flow air rates(v_{cf}): (a) the maximum flame height (H_{max}); (b) the minimum flame height (H_{min}); (c) the width of separated flame part (w_s).

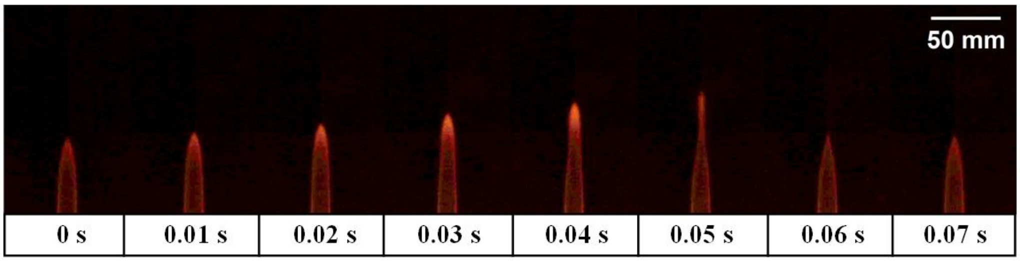

Fig. 11 A whole sequence of high-speed images of NH_3/CH_4 (α_N=0.3, with 10 slpm co-flow air) diffusion flames.

Images of the pure methane and NH_3/CH_4 diffusion flames are presented in Fig. 12. The pure methane diffusion flame has typical yellow and blue zones, while the addition of ammonia results in a reddish-orange flame that has no distinguishable zone. In contrast to the pure methane diffusion flame, the flame containing ammonia hardly shows noticeable changes in brightness during the flickering processes [36]. In order to highlight the changes in the flames, the variation of flame brightness at various ammonia ratio as function of time is presented in Fig. 13. The addition of ammonia greatly decreases the extent of the yellow emission, and the reddish-orange emission become dominant in the flame [31, 50]. The orange chemiluminescence results from the spectra of NH_2 α band and the super-heated water vapor [51]. There is a distinct brightness outline around NH_3/CH_4 diffusion flame. A conspicuous brightness appears at the separated part of the flame at α_N=0.3, whereas it is presented on the flame wings at α_N=0.5, where a brightness gradient can be observed. At α_N=0.3, the residual soot at the flame tip results in a brighter separated part. As stated in [52], the OH radical is primarily found on the flame wings, and play a key role in soot oxidation under fuel-rich conditions. With an increase in the amount of ammonia, the OH radical concentration decreases, and its distribution region narrows [53]. The reduction in amount of OH radicals leads to a small amount of soot remaining on the flame wings, which in turn forms a brightness gradient. A similar phenomenon was also observed by Najafi et al. [31]. They further investigated the chemiluminescence spectra of ammonia-methane flames. In pure methane flames, the blue emission zone was dominated by the excited states of CH and C_2 radicals, while the yellow zone was attributed to broadband soot emission. Ammonia substitution reduced the broadband emission intensity and introduced sharper spectral peaks, which corresponded to the NH_2 α band. As the ammonia fraction increased, the flame emission became dominated by the NH_2 α band with negligible broadband radiation observed.

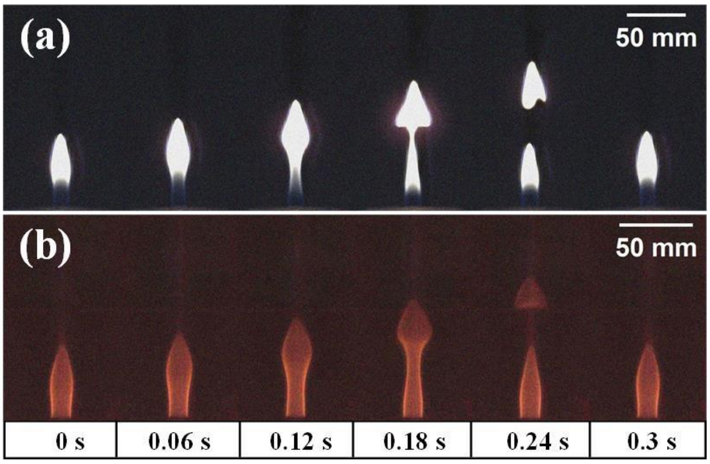

Fig. 12 Whole sequences of high-speed images of diffusion flames captured at 250 FPS: (a) methane (0.5 slpm); (b) NH_3/CH_4 (α_N=0.5).

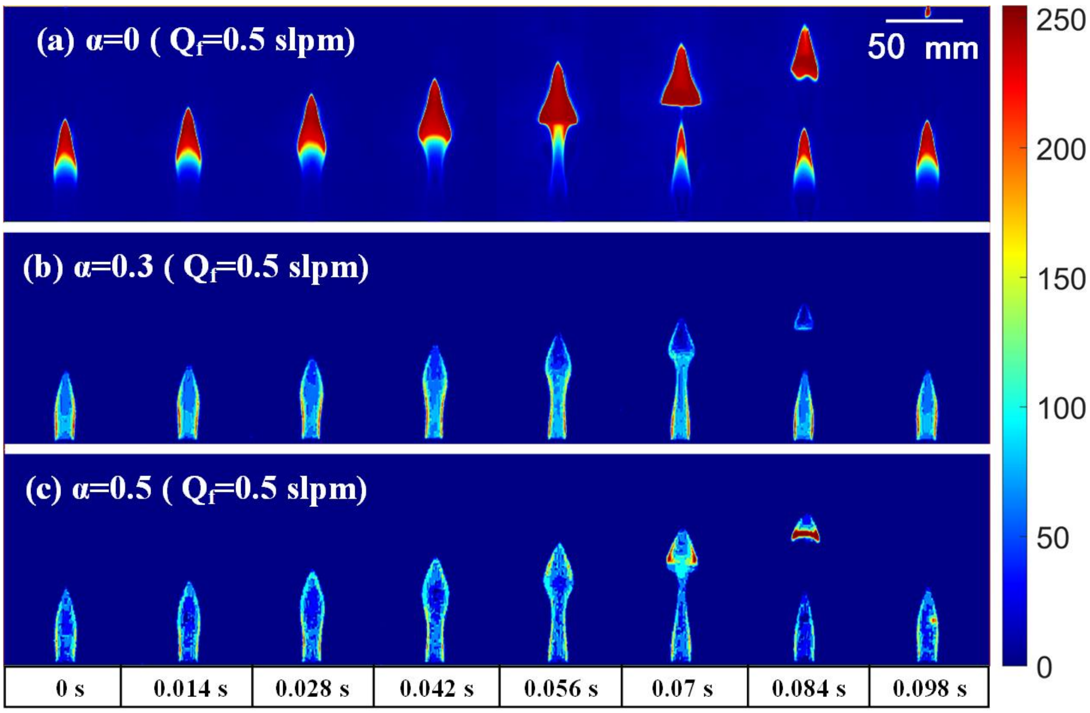

Fig. 13 The variation of flame brightness at various ammonia ratios over time.

3.2 Vortex structures

The schlieren method is widely used to investigate the generation and fortune of vortices around flames and its interaction with flame flickering [54, 55]. As found by Ge et al. [26], The flame flickering occurred only when the vortices formed at a lower position, and the vortices entrained reaction zone of flame. To further demonstrate the characteristics of flame flickering phenomenon, schlieren method was used in this study as well.

A complete sequence of schlieren images depicting the pure methane at 0.5 slpm without co-flow is presented in Fig. 14. The shear layer in the interface of flame and surrounding air presents a spindle shape, and conducts a periodic motion due to thermal expansion [56, 57]. As demonstrated in Fig. 14, the shear layer evolves along the following sequences: initially, a slight inward concavity, depicted by the yellow arrows in the images, occurs on the spindle-shaped shear layer. As time elapses, the concavity lifts, and develops into a vortex inside the shear layer according to the increasing diameter of the shear layer. In the meantime, the flame goes through a complete flickering cycle. The coinciding evolution of shear layer and flame flickering indicates that the motion of shear layer contributes to the bulge of the flame tip and the elongation of the region below the bulged. The vortex beneath the flame bulge pushes the surface of flame outward, while the vortex over the bulge pulls the surface inward [58]. The stretching even locally quenches an otherwise continuous flame surface, resulting in a separated flame [58]. Obviously, the flame flickering is significantly affected by the shear layer, both in appearance and frequency.

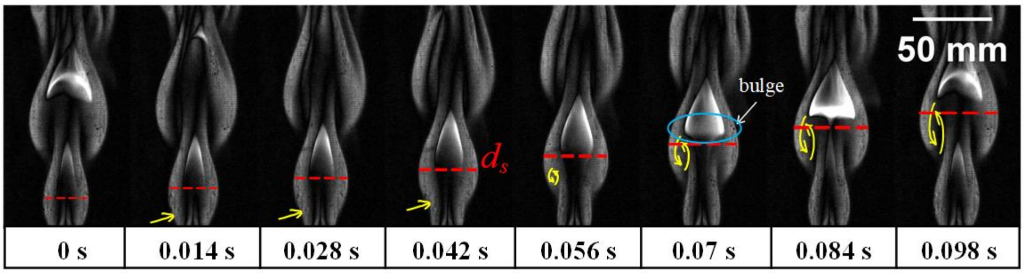

Fig. 14 Whole sequence of schlieren images for the pure methane at 0.5 slpm without additional co-flow.

The red dotted line shown in Fig. 14 represents the diameter of the shear layer (d_s), and the location of d_s is considered as the characteristic height of the current shear layer, which is used to calculate the motion velocity of the shear layer (v_s).The change in the d_s and v_s can be qualitatively used to describe the strength of the vortex [36]. The d_s over time for different fuels without co-flow is shown in Fig. 15. It is evident from Fig. 15(a) that the d_s expands with elapsed time for all Q_f, and ultimately reaches a constant value. The maximum value of d_s decreases with the diminished Q_f. With the addition of ammonia, d_s still increase with elapsed time, as shown in Fig. 15(b). The trend of d_s over time is not changed by the addition of ammonia. The expansion of shear layer is attributed to the continuous injection of the hot gas from the flame, which is less dense, into a reservoir of denser ambient air [59]. The shear layer, once away from the temperature field of the flame, stops expanding and may even shrink. During 0~0.056 s, the values of d_s for NH_3/CH_4 flame are comparable to that for the pure methane flame. After 0.056 s, there are obvious bifurcations, and the flame containing more ammonia possesses a lower d_s. As afore-discussed, the coinciding changes of d_s and w_s may be attributed to the reduction in the heat release by the addition of ammonia, accompanying with a lower flame temperature [6]. The reduced flame temperature leads to a decrease in the temperature gradient within the shear layer decreases, which in turn decreased density gradient and mass diffusion. Consequently, the reduced density gradient and mass diffusion result in the shrink of the shear layer [60].

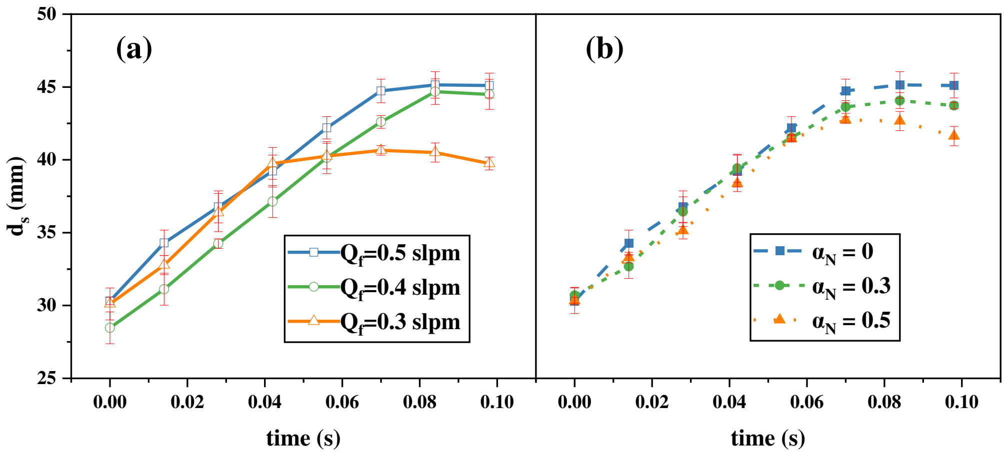

Fig. 15 Diameters of shear layer over time for different fuels without co-flow.

The v_s for different fuels is shown in Fig. 16. The v_s diminishes with elevated Q_f, whereas it increases with an increase in proportion of ammonia. The change of v_s with

Q_f is consistent with the change in f. Faster motion leads to a higher frequency. Interestingly, although v_s increases with the addition of ammonia, f does not increase monotonically. There may be other factors affecting the flickering behavior due to the presence of ammonia.

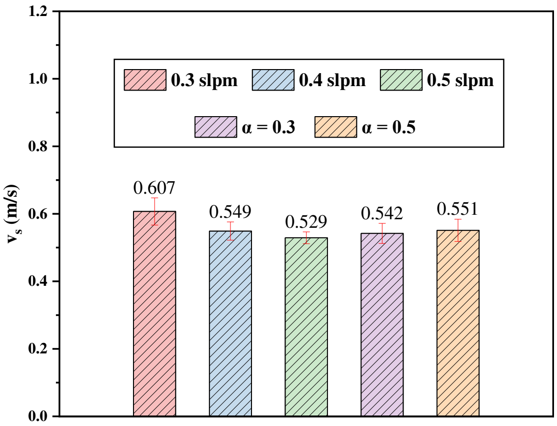

Fig. 16 The motion velocity of the shear layer (v_s) for various fuels.

As v_{cf} rises, the location of the vortex formation depicted by red arrow, elevates, as shown in Fig. 17. The fluctuation amplitude of the shear layer near the burner decreases and may even almost disappears. The result is consistent with the study of Gohari Darabkhani et al. [37] on a laminar methane diffusion flame. They found that the co-flow was prone to shift the location of the initial point of the vortices, and it then reached a stage where the vortices interacted solely with the hot gas stream beyond the visible flame region. The changed location of the vortex formation was also observed by Ge et al. [26] on a laminar methane diffusion flame with elevated pressure. They found that for a higher generation position of the vortices, the vortices did not impact the flame reaction zone, allowing the flame to remain stable. The flame flickering occurred only when the vortices were generated at a lower position, and the vortices entrained flame reaction zone. It can be concluded that when the location of the vortex formation is pushed beyond the visible flame region by the co-flow, the flickering is suppressed. To assess the position of the vortex formation, H_v is defined as the height at the location of the maximum d_s, when the second necking of the shear layer occurs, as depicted in Fig. 18. According to Fig. 19, H_v increases non-linearly with the increase in v_{cf} for all flames. When v_{cf} is <5 slpm, H_v for the NH_3/CH_4 flames is comparable to that for the pure methane flame. The NH_3/CH_4 flame is obviously larger than the pure methane flame in H_v with further increasing v_{cf}. Moreover, the increase rates of H_v of NH_3/CH_4 flame is greater than that of the pure methane flame. For α=0.5 with 10 slpm of v_{cf}, there are no fluctuation in the shear layer that tends to be cylindrical, as shown in Fig. 18. These findings suggested that the addition of ammonia promotes the downstream shift of the location of the vortex formation by the co-flow. It was speculated that the addition of ammonia decreased the upstream flame temperature, which in turn reduced the density gradient at the flame interface with the surrounding environment [33, 61]. As a result, the buoyancy-induced vortices around the flame were weakened. The shear layer became more susceptible to the co-flow air, and thus reducing the overall fluctuation intensity.

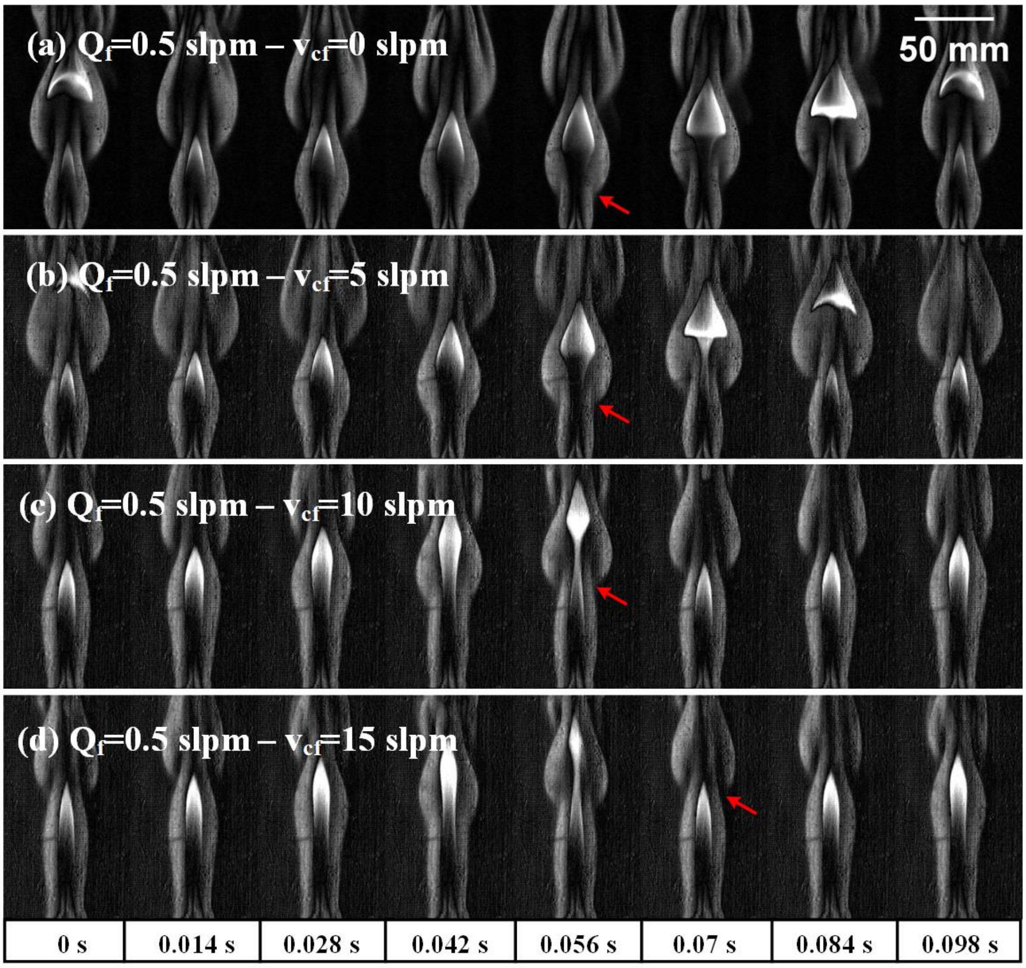

Fig. 17 Location of vortices formation (indicated by the red arrows) for the pure methane diffusion flame with various rates of co-flow air (v_{cf}).

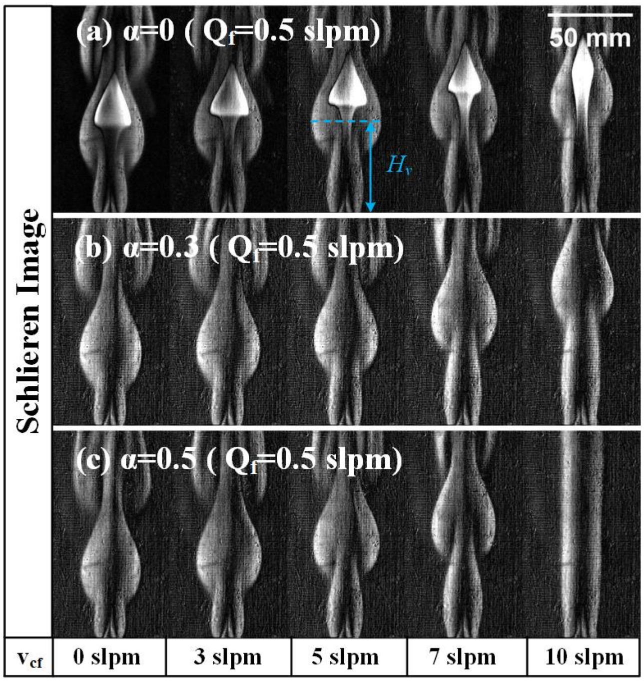

Fig. 18 Schlieren images of pure methane and NH_3/CH_4 diffusion flame at different rates of co-flow air (v_{cf}).

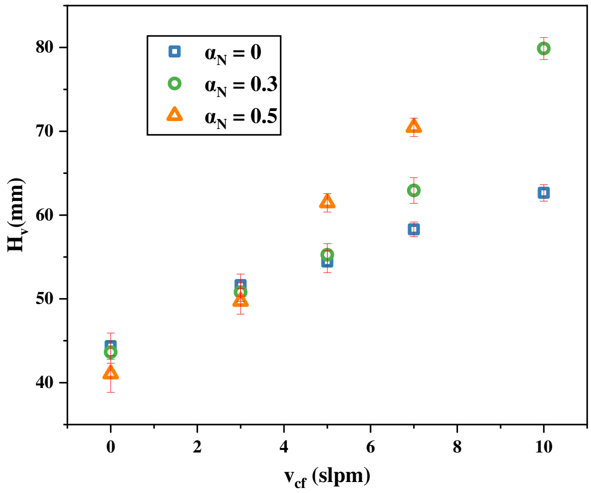

Fig. 19 Height of maximum diameter shear layer (H_v) for different flames at different rates of co-flow air (v_{cf}).

4. Conclusion

The effect of ammonia addition and co-flow air on the laminar methane jet diffusion flame were investigated experimentally by a high-speed camera system and schlieren method. In this study, with no additional co-flow gas, the threshold of Q_f for the stable flame is 0.16 slpm. When further elevating the Q_f, the flames possess regular and reproducible oscillation, accompanying with the periodic bulge and separation of the flame. The addition of co-flow leads to a higher flame flickering frequency that can be reduced by the increase in Q_f. The maximum height of flickering flames increases with v_{cf}, while the width of separation part decreases. The pure methane diffusion flame presents two typical luminous regions of partially-premixed region and diffusion (soot luminescence) region. The partially premixed region gradually stretches during flame flickering and increases with an increase in Q_f. In contrast, the NH_3/CH_4 diffusion flame presents a reddish-orange color and has no distinguishable luminous zone. Moreover, the addition of ammonia greatly shrinks the appearance of flames, and leads to a slight decrease in flame flickering frequency for 30% ammonia substitution whereas increase for 50% ammonia substitution. There is a spindle-shape shear layer between the flame and the surrounding air, conducting a periodic motion during the flickering sequence. The spindle-shape shear layer expands over time during the flame flickering, and eventually reaches a constant level. With the addition of ammonia, the maximum diameter of the shear layer decrease, and the motion velocity increases. As the addition of co-flow, the location of the vortex formation is pushed downstream, and the fluctuation amplitude of the shear layer near the burner decreases and may even almost disappear. The addition of ammonia further promotes the downstream shift of the location of the vortex formation by the co-flow, probably lessening the flame flickering. Apart from the presence of vortex, the heterogeneity of chemical kinetics in the flames is the main plausible factor related to flame flickering. Therefore, the chemical kinetics in the ammonia-containing laminar diffusion flames will be further investigated in our subsequent studies.

5. CRediT authorship contribution statement

Guorong Lin: Conceptualization, Investigation, Data visualization, Writing-original draft. **Chenyang Fan:** Investigation, Methodology, Funding acquisition, Project administration, Writing-review & editing. **Zheng Fu:** Investigation, Sources, Data visualization. **Haizhao Li:** Investigation, Data visualization; **Ye Liu**: Investigation, Data visualization. **Huiyong Du**: Methodology, Sources. **Bin Xu:** Methodology, Sources. **Shuo Jin:** Investigation, Data visualization, Validation. **Mingliang Wei**: Data Curation, Data visualization.

6. Conflicts of interest

The authors declare that they have no known competing financial interests or personal relationships that could have appeared to influence the work reported in this paper.

7. Acknowledgments

This research is sponsored by National Natural Science Foundation of China (No. 52006054), and International scientific and technological cooperation project in Henan Province (No. 232102521019).

8. Reference

[1] Al-Musleh EI, Mallapragada DS, Agrawal R. Continuous power supply from a baseload renewable power plant. Applied energy 2014;122:83-93.

[2] Kobayashi H, Hayakawa A, Somarathne KDKunkuma A, Okafor Ekenechukwu C. Science and technology of ammonia combustion. Proceedings of the Combustion Institute 2019;37(1):109-33.

[3] Dolan RH, Anderson JE, Wallington TJ. Outlook for ammonia as a sustainable transportation fuel. Sustainable Energy & Fuels 2021;5(19):4830-41.

[4] Jeerh G, Zhang M, Tao S. Recent progress in ammonia fuel cells and their potential applications. Journal of Materials Chemistry A 2021;9(2):727-52.

[5] del Pozo CA, Cloete S, Álvaro ÁJ. Ammonia from solid fuels: A cost-effective route to energy security with negative CO_2 emissions. Energy 2023;278:127880.

[6] Nonavinakere Vinod K, Gore M, Liu H, Fang T. Experimental characterization of ammonia, methane, and gasoline fuel mixtures in small scale spark ignited engines. Applications in Energy and Combustion Science 2023;16.

[7] Liang W, Law CK. Enhancing ammonia combustion using reactivity stratification with hydrogen addition. Proceedings of the Combustion Institute 2023;39(4):4419-26.

[8] Wang B, Wang H, Hu D, Yang C, Duan B, Wang Y. Study on the performance of premixed natural gas/ammonia engine with diesel ignition. Energy 2023;271:127056.

[9] Woo M, Choi BC. Numerical study on fuel-NO formation characteristics of ammonia-added methane fuel in laminar non-premixed flames with oxygen/carbon dioxide oxidizer. Energy 2021;226:120365.

[10] Okafor EC, Naito Y, Colson S, Ichikawa A, Kudo T, Hayakawa A, et al. Experimental and numerical study of the laminar burning velocity of CH_4–NH_3–air premixed flames. Combustion and Flame 2018;187:185-98.

[11] Huang F, Guo S, Wang L, Yang Z, Kong W. Experimental and numerical study on the performances of a free-piston engine generator using ammonia and methane fuel mixtures. Fuel 2023;341.

[12] Wei W, Li G, Zhang H, Wei F, Cai W, Dong D, et al. NOx generation in marine dual-fuel engines: Effects of ammonia blending ratio and spark ignition timing. Journal of Cleaner Production 2024;470:143332.

[13] Ariemma GB, Sorrentino G, Ragucci R, de Joannon M, Sabia P. Ammonia/Methane combustion: Stability and NOx emissions. Combustion and Flame 2022;241.

[14] Ku JW, Choi S, Kim HK, Lee S, Kwon OC. Extinction limits and structure of counterflow nonpremixed methane-ammonia/air flames. Energy 2018;165:314-25.

[15] Chu C, Scialabba G, Liu P, Serrano-Bayona R, Aydin FY, Pitsch H, et al. Effects of Ammonia Substitution in the Fuel Stream and Exhaust Gas Recirculation on

Extinction Limits of Non-premixed Methane– and Ethylene–Air Counterflow Flames. Energy & Fuels 2023;37(18):14393-403.

[16] Khateeb AA, Guiberti TF, Zhu X, Younes M, Jamal A, Roberts WL. Stability limits and exhaust NO performances of ammonia-methane-air swirl flames. Experimental Thermal and Fluid Science 2020;114.

[17] Joo HI, Gülder ÖL. Soot formation and temperature structure in small methane–oxygen diffusion flames at subcritical and supercritical pressures. Combustion and Flame 2010;157(6):1194-201.

[18] Liu F, Thomson KA, Guo H, Smallwood GJ. Numerical and experimental study of an axisymmetric coflow laminar methane–air diffusion flame at pressures between 5 and 40 atmospheres. Combustion and flame 2006;146(3):456-71.

[19] Peters N. Laminar diffusion flamelet models in non-premixed turbulent combustion. Progress in energy and combustion science 1984;10(3):319-39.

[20] Chamberlin D, Rose A. The flicker of luminous flames. *Proceedings of the Symposium on Combustion.* 1. Elsevier; 1948:27-32.

[21] Albers BW, Agrawal AK. Schlieren analysis of an oscillating gas-jet diffusion flame. Combustion and flame 1999;119(1-2):84-94.

[22] Lingens A, Neemann K, Meyer J, Schreiber M. Instability of diffusion flames. *Symposium (International) on Combustion.* 26. Elsevier; 1996:1053-61.

[23] Kimura I. Stability of laminar-jet flames. *Symposium (International) on Combustion.* 10. Elsevier; 1965:1295-300.

[24] Durox D, Yuan T, Villermaux E. The effect of buoyancy on flickering in diffusion flames. Combustion science and technology 1997;124(1-6):277-94.

[25] Zhang D, Fang J, Guan J-f, Wang J-w, Zeng Y, Wang J-j, et al. Laminar jet methane/air diffusion flame shapes and radiation of low air velocity coflow in microgravity. Fuel 2014;130:25-33.

[26] Ge Y, Li S, Wei X. Combustion states distinction of the methane/oxygen laminar co-flow diffusion flame at high pressure. Fuel 2019;243:221-9.

[27] Wang Q, Gohari Darabkhani H, Chen L, Zhang Y. Vortex dynamics and structures of methane/air jet diffusion flames with air coflow. Experimental Thermal and Fluid Science 2012;37:84-90.

[28] Piemsinlapakunchon T, Paul MC. Effect of syngas fuel compositions on the occurrence of instability of laminar diffusion flame. International Journal of Hydrogen Energy 2021;46(10):7573-88.

[29] Gohari Darabkhani H, Bassi J, Huang HW, Zhang Y. Fuel effects on diffusion flames at elevated pressures. Fuel 2009;88(2):264-71.

[30] Li J, Zhang Y. Fuel variability effect on flickering frequency of diffusion flames. Frontiers of Energy and Power Engineering in China 2009;3:134-40.

[31] Nourani Najafi SB, Mokhov AV, Levinsky HB. Investigation of the stability, radiation, and structure of laminar coflow diffusion flames of CH4/NH3 mixtures. Combustion and Flame 2022;244.

[32] Zhang F, Li S, Liu Q, Sun J, Wei X, Gu M, et al. Effect of ammonia on the soot

surface characteristics in ammonia/ethylene co-flow diffusion flames. Fuel 2023;341.

[33] Ren F, Cheng X, Gao Z, Huang Z, Zhu L. Effects of NH3 addition on polycyclic aromatic hydrocarbon and soot formation in C2H4 co-flow diffusion flames. Combustion and Flame 2022;241.

[34] Yan Z, Zhu T, Xue X, Liu H, Li Q, Huang Z. Effects of NH3 and H2 addition on morphology, nanostructure and oxidation of soot in n-decane diffusion flames. Fuel Processing Technology 2024;253.

[35] Colson S, Kuhni M, Hayakawa A, Kobayashi H, Galizzi C, Escudié D. Stabilization mechanisms of an ammonia/methane non-premixed jet flame up to liftoff. Combustion and Flame 2021;234.

[36] Yang X, Ma S, Gao J, Du Q, Zhang Y, Dong H. Suppression effect prediction of mixed combustion with ammonia under sub-atmospheric pressure on flicker of methane laminar diffusion flame. Energy 2024;298.

[37] Gohari Darabkhani H, Wang Q, Chen L, Zhang Y. Impact of co-flow air on buoyant diffusion flames flicker. Energy Conversion and Management 2011;52(8-9):2996-3003.

[38] Fujisawa N, Okuda T. Effects of co-flow and equivalence ratio on flickering in partially premixed flame. International Journal of Heat and Mass Transfer 2018;121:1089-98.

[39] Fujisawa N, Matsumoto Y, Yamagata T. Influence of Co-flow on Flickering Diffusion Flame. Flow, Turbulence and Combustion 2016;97(3):931-50.

[40] Wang Q, Mei XH, Wei ZY, Zhao CY, Zhang Y. Experimental investigation of transient ignition dynamics of hydrogen enriched methane diffusion impinging flames. Fuel 2021;290:120027.

[41] Wang Y, Yu Y, Zhu X, Zhang Z. Pattern recognition for measuring the flame stability of gas-fired combustion based on the image processing technology. Fuel 2020;270:117486.

[42] Richter H, Howard JB. Formation of polycyclic aromatic hydrocarbons and their growth to soot—a review of chemical reaction pathways. Progress in Energy and Combustion science 2000;26(4-6):565-608.

[43] Wang H. Formation of nascent soot and other condensed-phase materials in flames. Proceedings of the Combustion institute 2011;33(1):41-67.

[44] Zhang H, Yang Y, Li L, Peng Y, Xia X, Qi F. Frequency jump of a flickering buoyant jet diffusion flame influenced by ambient coflow. Proceedings of the Combustion Institute 2024;40(1-4).

[45] Lingens A, Reeker M, Schreiber M. Instability of buoyant diffusion flames. Experiments in Fluids 1996;20(4):241-8.

[46] Jiang X, Luo K. Combustion-induced buoyancy effects of an axisymmetric reactive plume. Proceedings of the combustion institute 2000;28(2):1989-95.

[47] Yang X, Ma S, Gao J, Du Q, Zhang Y, Dong H, et al. Mechanism and effect assessment of sub-atmospheric pressure and co-flow air to suppress the flicker

of buoyancy-driven methane laminar diffusion flame. Fuel Processing Technology 2023;242.

[48] Burke SP, Schumann TEW. Diffusion Flames. Industrial & Engineering Chemistry 1928;20(10):998-1004.

[49] Sato D, Davies J, Mazzotta L, Mashruk S, Valera-Medina A, Kurose R. Effects of Reynolds number and ammonia fraction on combustion characteristics of premixed ammonia-hydrogen-air swirling flames. Proceedings of the Combustion Institute 2024;40(1-4).

[50] Kim YH, Ku JW, Kwon OC. Combustion Characteristics for the Stabilization of Nonpremixed Methane-Ammonia/Air Coflow Flames through Their Visualization. Energy & Fuels 2024;38(10):9098-109.

[51] Hayakawa A, Goto T, Mimoto R, Kudo T, Kobayashi H. NO formation/reduction mechanisms of ammonia/air premixed flames at various equivalence ratios and pressures. Mechanical Engineering Journal 2015;2(1):14-00402-14-.

[52] Xu F, El-Leathy A, Kim C, Faeth G. Soot surface oxidation in hydrocarbon/air diffusion flames at atmospheric pressure. Combustion and flame 2003;132(1-2):43-57.

[53] Liu Y, Cheng X, Li Y, Qiu L, Wang X, Xu Y. Effects of ammonia addition on soot formation in ethylene laminar diffusion flames. Fuel 2021;292.

[54] Park J, Shin HD. Experimental investigation of the developing process of an unsteady diffusion flame. Combustion and flame 1997;110(1-2):67-77.

[55] Wang Q, Huang HW, Zhang Y, Zhao C. Impinging flame ignition and propagation visualisation using Schlieren and colour-enhanced stereo imaging techniques. Fuel 2013;108:177-83.

[56] Li D, Wen Y, Liu YC, Wang S. On the transition modes and mechanisms for laminar to turbulent lifted jet diffusion flames at normal- and micro-gravity. Combustion and Flame 2024;260.

[57] Law C. Dynamics of stretched flames. *Symposium (international) on combustion.* 22. Elsevier; 1989:1381-402.

[58] Chen L-D, Seaba J, Roquemore W, Goss L. Buoyant diffusion flames. *Symposium (international) on combustion.* 22. Elsevier; 1989:677-84.

[59] Wimer NT, Lapointe C, Christopher JD, Nigam SP, Hayden TRS, Upadhye A, et al. Scaling of the puffing Strouhal number for buoyant jets and plumes. Journal of Fluid Mechanics 2020;895.

[60] Mahesh Nayak G, Kolhe P, Balusamy S. Experimental study of buoyancy-induced instability in the DME and LPG jet diffusion flame. Fuel 2021;291.

[61] Ghoniem AF, Lakkis I, Soteriou M. Numerical simulation of the dynamics of large fire plumes and the phenomenon of puffing. *Symposium (International) on Combustion.* 26. Elsevier; 1996:1531-9.

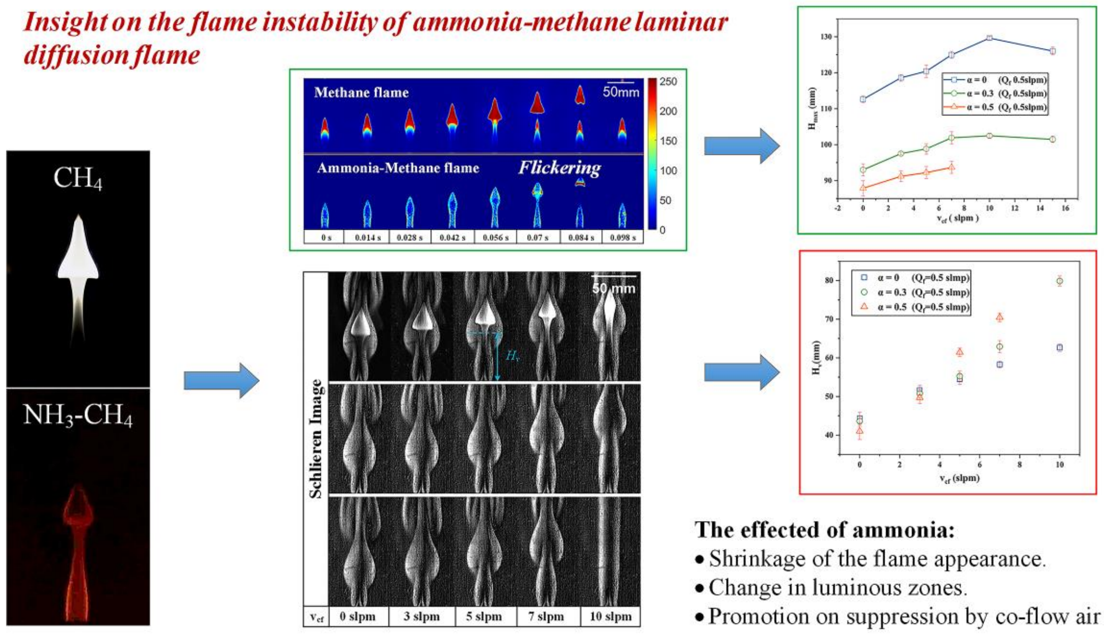

Insight on the flame instability of ammonia-methane laminar diffusion flame
CH4
NH3-CH4
Methane flame
50mm
Ammonia-Methane flame
Flickering
0 s
0.014 s
0.028 s
0.042 s
0.056 s
0.07 s
0.084 s
0.098 s
250
200
150
100
50
0
Schlieren Image
50 mm
vcf
0 slpm
3 slpm
5 slpm
7 slpm
10 slpm
The effected of ammonia:
• Shrinkage of the flame appearance.
• Change in luminous zones.
• Promotion on suppression by co-flow air